THE JOURNAL OF BIOLOGICAL CHEMISTRY
Vol. 278, No. 15, Issue of April 11, pp. 12903–12912, 2003
Printed in U.S.A.
© 2003 by The American Society for Biochemistry and Molecular Biology, Inc.

Identification of Oligomerization and Drug-binding Domains of the Membrane Fusion Protein EmrA*

Received for publication, September 16, 2002, and in revised form, December 6, 2002
Published, JBC Papers in Press, December 13, 2002, DOI 10.1074/jbc.M209457200

M. Ines Borges-Walmsley‡, Jeremy Beauchamp§¶, Sharon M. Kelly‖, Kornelia Jumel, Denise Candlish§, Stephen E. Harding**, Nicholas C. Price‖, and Adrian R. Walmsley‡ ‡‡**

*From the ‡Centre for Infectious Diseases, Wolfson Research Institute, University of Durham, Queen's Campus, Stockton-on-Tees, TS17 6BH, §Division of Infection and Immunity and ‖Division of Biochemistry and Molecular Biology, Institute of Biomedical and Life Sciences and ¶Department of Chemistry, University of Glasgow, Glasgow G11 6NU, and the **National Center for Macromolecular Hydrodynamics, School of Biosciences, University of Nottingham, Sutton Bonington LE12 5RD, United Kingdom*

Many pathogenic Gram-negative bacteria possess tripartite transporters that catalyze drug extrusion across the inner and outer membranes, thereby conferring resistance. These transporters consist of inner (IMP) and outer (OMP) membrane proteins, which are coupled by a periplasmic membrane fusion (MFP) protein. However, it is not know whether the MFP translocates the drug between the membranes, by acting as a channel, or whether it brings the IMP and OMP together, facilitating drug transfer. The MFP EmrA has an elongated periplasmic domain, which binds transported drugs, and is anchored to the inner membrane by a single α-helix, which contains a leucine zipper dimerization domain. Consistent with CD and hydrodynamic analyses, the periplasmic domain is predicted to be composed of a β-sheet subdomain and an α-helical coiled-coil. We propose that EmrA forms a trimer in which the coiled-coils radiate across the periplasm, where they could sequester the OMP TolC. The "free" leucine zipper in the EmrA trimer might stabilize the interaction with the IMP EmrB, which also possesses leucine zipper motifs in the putative N- and C-terminal helices. The β-sheet subdomain of EmrA would sit at the membrane surface adjacent to the EmrB, from which it receives the transported drug, inducing a conformational change that triggers the interaction with the OMP.

A major mechanism of resistance in pathogenic bacteria is the extrusion of antibiotics from the cell. Gram-negative bacteria possess tripartite transport systems for translocating drugs across both the inner membrane (IM)[1] and the outer membrane (OM). This system consists of inner and outer membrane proteins, which translocate drugs across their respective membranes but are coupled by a periplasmic protein (1). The periplasmic domain of this protein is apparently anchored to the IM via either a lipid moiety or an α-helix. There has been much speculation as to the functional role of this periplasmic protein, the delineation of which is crucial to understanding the mechanism of this type of transport system. One proposal is that it forms a channel between the membranes; but another suggests that it pulls the membranes together, allowing ligand transfer between the IMP and OMP (2). Because of the latter hypothesis this periplasmic protein was originally termed a membrane fusion protein (MFP), but more recently the term dynamic adaptor has been adopted (3).

The structures of two of the components of such a tripartite complex, the OMP TolC (4) and the IMP AcrB (5), have recently been determined by x-ray crystallography (4). Both TolC and AcrB crystallize as trimers. The three TolC molecules are structured into a 140-Å cylindrical channel with a 35-Å internal diameter. The OM end of the structure is open, providing solvent access, but the periplasmic end tapers to a virtual close. The structure can be divided into two major domains: an OM β-barrel and a periplasmic α-helical barrel. The β-barrel domain, which provides an essentially open channel through the OM, is composed of 12 β-strands, 4 donated by each TolC molecule, arranged into a right-twisted barrel. The α-helical domain is a 12-helix barrel, constructed from long (67 residues) and short (23 and 34 residues) helices, with pairs of the shorter helices stacked to produce pseudo-continuous helices. The α-helices are further arranged into coiled-coils, and the mixed α/β structure connecting the shorter helices forms a belt around the helical barrel. The α-helical barrel is about 100 Å long, which is close to the lower estimates of the depth of the periplasmic space at 130 Å, but some estimates put the depth of the periplasm at 250 Å and beyond the span of TolC (6, 7). The AcrB trimer, which has a jellyfish-like appearance, comprises a periplasmic headpiece with dimensions of 50 × >100 Å and a transmembrane domain with dimensions of 70 × >80 Å (5). The headpiece, which is formed by protrusions between helices 1 and 2 and helices 7 and 8 of the transmembrane domain, is divided into two stacked parts, with the upper and lower parts 30 and 40 Å thick, respectively. Viewed from the side, the upper part has a trapezoidal appearance, 70 Å wide at

* This work was supported by grants from the Biotechnology and Biological Sciences Research Council (BBSRC) and Wellcome Trust (to A. R. W.). The CD facility at the University of Glasgow and the National Center for Macromolecular Hydrodynamics at the University of Nottingham are both supported by the BBSRC and the Engineering and Physical Sciences Research Council (EPSRC). The costs of publication of this article were defrayed in part by the payment of page charges. This article must therefore be hereby marked "*advertisement*" in accordance with 18 U.S.C. Section 1734 solely to indicate this fact.

‡‡ To whom correspondence should be addressed: Centre for Infectious Diseases, Wolfson Research Institute, University of Durham, Queen's Campus, Stockton-on-Tees TS17 6BH, United Kingdom. Tel.: 44-1642-333836; Fax: 44-1642-333817; E-mail: a.r.walmsley@durham.ac.uk.

[1] The abbreviations used are: IM, inner membrane; MFP, membrane fusion protein; IMP, inner membrane protein (a membrane transporter); CB, carbenicillin; MES, 4-morpholineethanesulfonic acid; MIC, minimum inhibitory concentration; MOPS, 4-morpholinepropanesulfonic acid; NTA, nitrilotriacetic acid; OM, outer membrane; OMP, outer membrane protein (an α/β-barrel protein channel); RND, resistance-nodulation-cell division family of membrane transporters; FCCP, carbonyl cyanide *p*-trifluoromethoxyphenyl-hydrazone; CCCP, carbonyl cyanide *m*-chlorophenyl-hydrazone; DNP, 2,4-dinitrophenol.

Downloaded from http://www.jbc.org/ at DURHAM UNIVERSITY on August 29, 2017

the bottom and 40 Å at the top; whereas viewed from above, the upper part is open like a funnel, with an internal diameter of 30 Å. This funnel is connected by a pore, located between the headpieces of the three protomers, to a large central cavity at the interface of the headpiece and the transmembrane domains of the protomers. The three transmembrane domains, each of which is composed of 12 helices, are arranged into a ring with a 30-Å hole between them, which might be filled with phospholipids. It has been proposed that the upper headpiece interacts with TolC (5), with six vertical hairpins from the AcrAB trimer contacting the six α-helix-turn-α-helix structures of the TolC trimer, to form a continuous path across the periplasmic space. If this is the case, it suggests a mechanism in which drugs transported through the transmembrane domains of AcrB are delivered to the central cavity created at the transmembrane domain headpiece interface, where they can be shuttled through the headpiece pore and funnel to TolC.

Interestingly, MFPs are predicted to have a structure that resembles TolC; the N- and C termini of MFPs are proposed to fold into a flattened β-barrel, with the intervening residues arranged into two long helices, each of about 60 or more residues, which fold back on one another to form a coiled-coil (2). Considering those MFPs that utilize an N-terminal α-helix to anchor them to the IM, this would position the β-barrel at the IM with the α-helices radiating out across the periplasm. Furthermore, the ability of MFPs to form stable trimers (8, 9) invites the suggestion that their role is to form a connecting channel between the IM translocase and TolC. The putative β-barrel of the MFP could act as the receiver domain for drugs released from the IM translocase, whereas the α-helices could transiently interact with TolC. A possible mechanism for this interaction is that the six α-helices of the MFP trimer form a cylinder that inserts into the closed end of TolC to open it. Considering however that both TolC and MFPs are highly elongated molecules (4, 9) capable of overlapping in the periplasmic space, a more likely mechanism is for the MFP to utilize its α-helices to "grab" the outer surface of TolC. There is a deep cleft within the headpiece of AcrB in which the MFP AcrA may lie, thereby positioning it to straddle both the periplasmic domains of AcrB and TolC (5), and biochemical cross-linking studies have revealed that the MFP-TolC interaction is substrate-induced and transient (8). On the other hand, the β-domain contains a motif that resembles the lipoyl domain of enzymes involved in the transfer of a covalently attached lipoyl or biotinyl moiety between proteins (2). In such enzymes, this lipoyl domain is usually a flattened β-barrel. The formation of a similar domain would require the N- and C-terminal domains of the MFP to interact, which might provide a mechanism for bringing the two membranes together. However, the dimensions of AcrB and TolC are sufficient to indicate that they can contact one another across the periplasm, arguing against a role for the MFP in bringing the IM and OM together.

This type of transport system is clearly of considerable scientific and medical interest, because our knowledge of them is rudimentary, and their study is likely to have medical benefits, because they confer drug resistance and only effect transport in bacteria. For this study, our aim was to characterize EmrA, the MFP of a multidrug transporter from *Escherichia coli* (10), as a structural and functional paradigm for the elucidation of the properties of a number of IMP-MFP-OMP transport systems and to address the central question of the role of the MFP in drug translocation. The EmrAB transporter is composed of EmrB, a putative 14-helix multidrug H^+ antiporter belonging to the major facilitator (MF) superfamily (11), and the MFP EmrA. EmrA is predicted to have a short N-terminal cytoplasmic domain, a single transmembrane helix, and a large periplasmic domain. The EmrAB proteins are thought to provide a continuous pathway across the bacterial membranes by operating in conjunction with TolC (1). Underscoring the medical importance of this system, homologues of EmrA and B have been found in human pathogenic bacteria such as *Vibrio cholerae* (12), *Neisseria gonorrhoeae* (13), *Strenotrophomonas maltophilia* (14), and *Campylobacter jejuni* (15). Also the genome sequences of *Bacillus subtilis*, *Haemophilus influenzae*, *Neisseria meningitidis*, *Bordatella pertussis*, *Rickettsia prowazeki*, and *Yersinia pestis* indicate that they possess related systems.

MATERIALS AND METHODS

Bacterial Strains and Plasmids—The pGEM-Teasy (Promega) plasmids bearing the *emrA* inserts were propagated in NovaBlue *E. coli* cells (Novagen). The pET21 (Novagen) plasmid constructs bearing *emrA* inserts were propagated in *E. coli* strain C41, a derivative of BL21 (16), and that bearing the *hmrA* insert was propagated in BL21* (Invitrogen). A Δ*acrA* strain of *E. coli*, termed N43 (17), was transformed with *E. coli emrAB*, Δ*NTemrAemrB* (*i.e.* the construct expressed EmrA-(49–390)), and *H. influenzae hmrAB* pUC constructs and used for MIC measurements.

Overexpression and Purification of His-tagged EmrA Proteins—Chromosomal DNA from *E. coli* strain DH5α was used as target DNA for amplification of *emrA* by PCR using the forward and reverse oligonucleotide primers 5′-GGATCCAGCGCAAATGCGGAGACTCA-3′ and 5′-CTCGAGGCCAGCGTTAGCTTTTACGAT-3′, respectively. We incorporated *Bam*HI and *Xho*I restriction sites (underlined) into these primers to allow fragment ligation into pET21a to produce construct pET-EmrA-(1–390). Four truncated fragments of EmrA were generated by PCR, *emrA*-(15–390), *emrA*-(29–390), and *emrA*-(49–390), with the forward primers 5′-GGATCCAAGAGCGGCAAACGTAAG-3′, 5′-GGATCCCTCTTTATAATTATTGCCGT-3′ and 5′-GGATCCGAAGAAACCGATGACGCATACG-3′, respectively, in combination with the reverse primer used to clone *emrA*-(1–390), whereas *emrA*-(1–56) was generated with the forward primer used to clone *emrA*-(1–390) and the reverse primer 5′-CTCGAGCGTATGCGTCATCGGTTTCTTC-3′. In each case *Bam*HI-*Xho*I restriction fragments were prepared and ligated into pET21a to produce constructs pET-EmrA-(15–390), pET-EmrA-(29–390), pET-EmrA-(49–390), and pET-EmrA-(1–56). Each pET construct was sequenced to ensure its integrity and that it was in-frame with the T7 and His_6 tags.

The pET constructs were used to transform *E. coli* strain C41, providing expression of the His_6-tagged proteins. A single colony of C41/pET-EmrA was used to inoculate 5 ml of tryptone-yeast extract/50 μg ml^{-1} carbenicillin (CB), grown to saturation at 37 °C, and used to inoculate 0.5 liters of tryptone-yeast extract/50 μg ml^{-1} CB. Growth was continued at 37 °C until reaching an A_{600} of 0.4–0.5, at which point 1 mM isopropyl-1-thio-β-D-galactopyranoside/50 μg ml^{-1} CB was added, and the growth continued overnight at a reduced temperature of 23 °C. For most preparations 3 liters of cells (*e.g.* 6 × 0.5 liters) were cultivated. Cells were harvested at 8670 × *g* and washed with TNG buffer (50 mM Tris-HCl (pH 8.5), 150 mM NaCl, 10% glycerol). The cell pellet from each 0.5-liter culture was resuspended in 20 ml of TNG buffer, giving 100 ml for a 3-liter culture, to which was added 0.5 ml 10 mg ml^{-1} lysozyme, 0.1 ml 10 mg ml^{-1} DNase, and 1 protease inhibitor mixture tablet (complete, EDTA-free™, Roche Molecular Biochemicals). The cells were disrupted by passage through a cell disrupter (model Z-plus 1.1 kilowatts, Constant Systems) operated at 4 °C. Unbroken cells and cell debris were cleared from the supernatant at 39,000 × *g* (20 min, 4 °C), which was then spun at 194,000 × *g* (1.5 h, 4 °C), separating the soluble protein from the cell membrane pellet. EmrA-(49–390) was isolated from the supernatant, EmrA-(1–56), EmrA-(15–390), and EmrA-(1–390) from the membranes, and EmrA-(29–390) from both the membrane and soluble fractions. For purification of EmrA-(49–390), 6 ml of suspended Ni^{2+}-NTA-agarose (Qiagen) was added to one-quarter of the supernatant and incubated for 1 h at 4 °C. A 1.5-cm-diameter Econo-column™ (BioRad) was packed with the Ni^{2+}-NTA-agarose to a final column volume of about 3 ml and washed successively with 10, 2.5, and 0.5 volumes of TNG buffer containing 10, 25, and 50 mM imidazole, respectively, before elution of the protein under gravity with 400 mM imidazole in 50 mM Tris-HCl (pH 8.5), 200 mM KCl (TK). Generally, 5 ml of protein at 15–20 mg ml^{-1} was eluted from the column, and then a further 5 ml of protein at 5 mg ml^{-1} was eluted, thus giving a yield of about 400 mg of protein from a 3-liter culture. The protein was dialyzed against TK to remove the imidazole.

Downloaded from http://www.jbc.org/ at DURHAM UNIVERSITY on August 29, 2017

EmrA-(29–390) was obtained from the soluble fraction in an identical manner. For EmrA-(1–390), EmrA-(1–56), EmrA-(15–390), and EmrA-(29–390) (membrane fraction) purifications, each membrane pellet was solubilized by the addition of 1 volume of 1.5% dodecyl-β-D-maltoside in TKG buffer (TK plus 10% glycerol) and incubated on ice for 1 h, after which time 9 volumes of TKG was added to reduce the dodecyl-β-D-maltoside concentration to 0.15%, and solubilized proteins were separated from the membrane debris at 194,000 × *g*. To 100 ml of supernatant, 4 ml of suspended Ni^{2+}-NTA-agarose/1 protease inhibitor tablet was added and incubated for 3 h at 4 °C. A 1-cm-diameter Econo-column was packed with the Ni^{2+}-NTA-agarose to a final volume of about 2 ml and washed successively with 10, 2.5, and 2 volumes of TKGN (TKG plus 0.2% *n*-nonyl-β-D-maltoside) containing 10, 25, and 50 mM imidazole, respectively. 400 mM imidazole/TKGN was used to elute the protein under gravity, with the protein usually occurring in the second and third 1-ml aliquot at a concentration of 0.5–1 mg ml^{-1}. The protein was dialyzed against TKGN to remove the imidazole.

Each pET-EmrA construct was tested for expression in the cytoplasm, inner membrane, and periplasm by purification. Proteins were released from the periplasm by cold osmotic shock of the cells (18), and the protein extract was treated according to the procedure adopted for the purification of soluble EmrA proteins but maintaining the proteins in glycerol-containing buffers. Proteins were quickly frozen and stored at −80 °C.

Overexpression and Purification of the His-tagged HmrA Protein—H. influenzae Rd, KW20, genomic DNA was obtained from the American Type Culture Collection and used to PCR clone the periplasmic domain of HmrA, the *H. influenzae* homologue of EmrA, with the primers 5′-CACCATGTTTGAAGAAACAGAAGATGCTTATGTGG-3′ and 5′-ATGGCTGTTTTTGCTGAATGATAGATTC-3′. The resulting product was cloned into the pET101/D-TOPO (Invitrogen) expression vector giving the pHmrA-6H plasmid, which was used to transform *E. coli* TOP10 cells, for overexpression of HmrA-(48–390). Automated DNA sequencing of the plasmid confirmed the sequence and translation frame as correct. pHmrA-6H was used to transform *E. coli* BL21* (Invitrogen), which was used for all subsequent protein production.

BL21*/pHmrA-6H cells were grown at 37 °C in a 10-ml LB starter culture containing 100 μg/ml carbenicillin from a single colony picked from a fresh agar plate. When the cells were just visible, 1 ml of starter culture was used to inoculate 1 liter of LB containing 100 μg/ml CB, which was grown to an A_{600} of 0.4 at 37 °C with shaking at 200 rpm. Cells were induced with 1 mM isopropyl-1-thio-β-D-galactopyranoside for 3 h at 25 °C and then chilled on ice for 1 h. The cells were harvested by centrifugation, resuspended in 50 mM HEPES (pH 8.0), 300 mM KCl, and disrupted with a Cell Disrupter (Constant Systems). The cell debris was removed by centrifugation and frozen in five 25-ml aliquots at −80 °C. HmrA-(48–390) was purified according to the same protocol adopted for EmrA-(49–390).

Construction of pUC-EmrAB, pUC-EmrA-(49–390)B and pUC-HmrAB—The *emrA* and *emrB* genes were amplified by PCR using the forward and reverse primers 5′-GAATTCGAGCGCAAATGCGGAGACTC-3′ and 5′-GAAGCTTAGTGCGCACCTCCGCC-3′, respectively, to introduce *Eco*RI and *Hin*dIII sites (underlined) at the 5′ and 3′ ends of the amplified DNA, which was purified and ligated into pGEMT-Easy (Promega). The *emrAB* genes were rescued from pGEM-Teasy by restriction digest with *Eco*RI and *Hin*dIII, ligated into *Eco*RI/*Hin*dIII-digested pUC to create pUC-EmrAB, and transformed into *E. coli* strain N43. Similarly, the pUC-EmrA-(49–390)B construct was made using the forward primer 5′-GAATTCGAAGAAACCGATGACGCATACG-3′, so that the expressed EmrA lacked the first 48 amino acids. The constructs were checked by automated DNA sequencing. The *hmrA* and *hmrB* genes were amplified by PCR using the forward and reverse primers 5′-GAATTCTGACGCAAATTGCAACT-3′ and 5′-GAAGCTTAATGCTGAGTACC AAA-3′, respectively. The PCR product was purified and ligated into pGEM-Teasy (Promega). The *hmrAB* genes were rescued from pGEM-Teasy by restriction digest with *Eco*RI, ligated into *Eco*RI-digested, alkaline phosphatase-treated pUC to create pUC-HmrAB, and transformed into *E. coli* (NovoBlue, Invitrogen). Automated DNA sequencing was used to identify a plasmid in which the *hmrAB* genes were correctly orientated, which was then used to transform strain N43.

MIC Measurements—MICs were measured according to the microdilution broth method established by the National Committee for Clinical Laboratory Standards (19). Briefly, a single colony was picked from an LB/ampicillin plate, used to inoculate 20 ml LB/ampicillin medium, and grown to an A_{600} of 0.1. Cells were transferred to a microtiter plate and mixed with serial dilutions of the drug to be tested. Bacterial growth was monitored after an 18-h incubation at 37 °C.

Protein Concentration and Gel Analysis—Protein concentrations were determined by the BCA assay using a kit from Pierce with bovine serum albumin as standard. Proteins were separated by SDS-PAGE on 4–12% or 12% polyacrylamide gradient gels (NuPAGE gels and MES or MOPS buffer; Novex) and stained with Coomassie Gelcode Blue™ (Pierce). Protein samples for SDS-PAGE were mixed with the loading buffer at room temperature to avoid any potential problems due to protein aggregation, which can occur when samples are boiled. Native PAGE (7.5% (BioRad) polyacrylamide gels and Tris-glycine buffer (pH 7.5) run for 16 h at 50 v) was also used to separate proteins.

Gel Chromatography—EmrA proteins were subjected to gel chromatography on a Superdex 200 column run on an AKTA purifier (Amersham Biosciences) automated chromatography system. EmrA-(1–390) (1.3 mg ml^{-1} in TKGN) and EmrA-(49–390) (3.0 mg ml^{-1} in TKG) were applied to a Superdex 200 HR 10/30 column equilibrated with PNGL buffer (25 mM sodium phosphate (pH 8.0), 150 mM NaCl, 10% glycerol, 0.1% lauryldimethylamine-*N*-oxide) and eluted at a flow rate of 0.25 ml min^{-1}. It was necessary to utilize PNGL as the equilibration buffer because the separation of the monomers and dimers of EmrA was inefficient when TKGN was used as the equilibration buffer, which however is better for storage of EmrA. Although the retention time for the EmrA-(49–390) monomer appeared to be less than for the EmrA-(1–390) dimer and monomer, possibly because the proteins adopt different conformations, the column resolution would be relatively poor in this range (*e.g.* between 45 and 90 kDa), and consequently there would be difficulties in comparing the elution profiles from different runs. Accordingly, we did not try to estimate the molecular masses of the proteins from the retention times. Moreover, the proteins are likely to elute as protein-detergent micelles with a greater molecular mass than the protein.

Western Blotting and N-terminal Sequencing—EmrA-(1–390) monomers and dimers were separated by gel chromatography on a Superdex 200 column, resolved by 12% SDS-PAGE, transferred to polyvinylidene difluoride membrane and either immunoblotted with monoclonal anti-polyhistidine antibodies (Sigma) or N-terminal sequenced (Alta Bioscience, University of Birmingham, UK). The predicted amino acid sequence of the EmrA-(2–390)-$(His)_6$ fusion protein (*i.e.* termed EmrA-(1–390)) was MASMTGGQQMGRDP-EmrA-(2–390)-LEHHHHHH, with residues 2–12 constituting an immunogenic T7 tag. N-terminal sequencing of the EmrA-(1–390) gave the first 11 and 10 residues of the T7 tag for the monomer and dimer, respectively.

Spectroscopic Analyses—CD spectra were recorded on a Jasco J600 spectrometer at 20 °C using protein samples dialyzed into 50 mM Tris-acetic acid (pH 8.0), 200 mM NaF. The percentage of secondary structure was predicted from the CD spectra using the program SELCON (20).

Fluorescence measurements were made in a Jasco FP750 fluorimeter at 20 °C. Tryptophan fluorescence was excited at 292.5 nm, and the emission wavelength was scanned between 300 and 400 nm. For titrations of EmrA-(49–390), KI was added from a 5 M stock solution to 2 ml of 1.25 μM protein in 50 mM Tris-HCl (pH 8.5), 200 mM NaCl. For KI titrations in the presence of drugs, the drug concentration was set to the maximum possible (*e.g.* 39 μM FCCP, 48 μM CCCP, 19 μM DNP, 20 μM nalidixic acid, and 53 μM chloramphenicol) that would not reduce the protein fluorescence by more than 50% because of its inner filter effect. In the case of nalidixic acid, the pH of the protein solutions was tested to ensure that the small volume of acid added had not perturbed the pH. The protein fluorescence and KI concentration were corrected for the dilution effect. HmrA-(48–390) was routinely used at a concentration of 6 μM because this gave a fluorescence equivalent to 1.25 μM EmrA-(49–390), but using the proteins at equivalent concentrations did not affect the titration curves. The FCCP titration curve for EmrA was fitted to an equation with hyperbolic and linear functions by nonlinear regression using the program SigmaPlot (Jandel Scientific): $y = A - [(B \times [FCCP]/K_d + [FCCP]) + (C \times [FCCP])]$, where A is the value of F_0/F in the absence of FCCP, B is the total decrease in the value of F_0/F for concentrations of FCCP that tend toward saturating the hyperbolic component attributed to specific binding, K_d is the dissociation constant for the specific EmrA-(49–390)-FCCP complex, and C is the slope of the linear component attributed to nonspecific binding.

Analytical Ultracentrifugation—Sedimentation velocity and sedimentation equilibrium measurements were made with an Optima XL-A analytical Ultracentrifuge (Beckman). Sedimentation was performed at 45,000 rpm in double sector cells at 20 °C, and the data were analyzed using DCDT+ software, version 1.12 (21). We measured the value of s for different protein concentrations in the range of 0.5–1 mg/ml in 40 mM potassium phosphate (pH 8.0), 400 mM KCl and extrapolated the data to zero protein concentration. Sedimentation equilibrium experiments were performed at 15,000, 18,000 and 20,000 rpm at 20 °C, and the data were analyzed using the manufacturer's software (Microcal

Downloaded from http://www.jbc.org/ at DURHAM UNIVERSITY on August 29, 2017

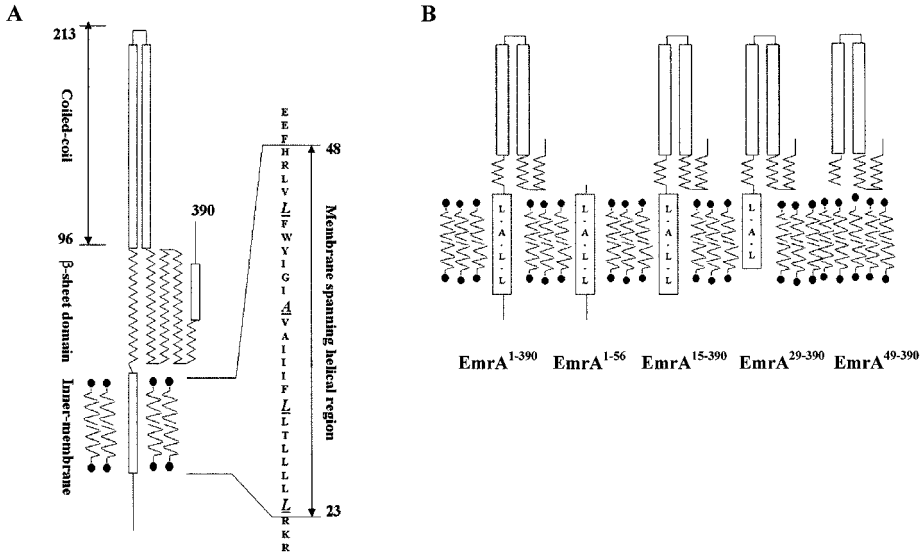

FIG. 1. **Schematic diagram of EmrA based upon the predicted secondary structure and domain mapping experiments.** *A*, schematic model of the EmrA secondary structure. The amino acid sequence surrounding the N-terminal α-helix that anchors EmrA to the inner membrane is shown, indicating the positions of the truncated EmrA constructs (in *B*) used to map the EmrA domains. Those residues belonging to a putative leucine zipper motif, which runs through the α-helix, are *underlined* and *italic*. *B*, predicted topologies of the truncated derivatives of EmrA constructed to map the domains of EmrA. The α-helices and β-sheet domains are shown as *rectangles* and *saw-tooth* schematics, respectively. The *letters* in the membrane-spanning helix represent the leucine zipper motif; note that this is truncated in EmrA-(29–390).

Origin, version 4.1). The partial specific volume, $\tilde{v}$, was calculated as 0.736 ml/g from the amino acid sequence of EmrA-(49–390) using SEDNTERP software (22); this value was used in all calculations.

Dynamic Light Scattering—Dynamic light scattering experiments were performed on a Dynapro 801 (Protein Solutions Inc.) instrument at 20 °C. Samples were injected at a concentration of 1 mg ml^{-1}. Data analysis was performed using the manufacturer's software.

RESULTS

EmrA Has a Periplasmic Domain That Is Anchored to the Membrane by a Single α-Helical Domain—Residues 23–46 of EmrA were predicted, using the program TMHMM (23), to form an α-helix that anchors the protein in the periplasm of *E. coli*. However, this prediction for EmrA, or for any other MFP, has not been tested experimentally. To map the domains of EmrA, a number of *emrA* constructs were made in pET to overexpress the whole and truncated portions of EmrA (Fig. 1) with a His tag to aid in purification (Fig. 2*A*). To determine the location of each protein, we attempted their purification from the periplasm milieu, obtained by osmotic shock of the cells, from the cytoplasmic milieu, obtained as the soluble fraction after cell disruption, and from inner membranes, prepared by detergent solubilization of membranes from disrupted cells. The EmrA-(1–390), EmrA-(15–390), and EmrA-(1–59) proteins were purified from cytoplasmic membranes, whereas EmrA-(49–390) was purified as a soluble protein from the cytoplasm. In contrast, EmrA-(29–390) was obtained from both membranes (about two-thirds of the total protein) and the cytoplasm (about one-third of the total protein). None of the proteins was purified from the periplasmic milieu following osmotic shock. We concluded that EmrA is anchored to the membrane by residues 15–49.

EmrA Forms Dimers and Trimers—An analysis of the EmrA-(1–390) protein by SDS-PAGE (4–12% polyacrylamide gel, MES buffer) revealed two predominant bands, one migrating close to the expected molecular mass of 45.1 kDa and the other with an apparent molecular mass of about 60 kDa (Fig. 2*A, lane 5*). Similarly, two predominant bands were apparent for the truncate EmrA-(15–390), but both bands ran slightly faster than the corresponding bands for EmrA-(1–390) (Fig. 2, *A*, *lane 4*, and *B*). This suggested that the higher molecular mass bands were dimers of EmrA that ran at a lower than expected molecular mass, as is usually the case for membrane proteins. However, better resolution of the dimer molecular mass was obtained under alternate SDS-PAGE conditions (12% gel, MOPS buffer), indicating that the dimer has a molecular mass in excess of 64 kDa (Fig. 2*B*, *lane 2*). It seems unlikely that these high molecular mass bands are attributable to complexes with other proteins, such as EmrB and TolC, because their intensity is much greater than would be expected when considering the wild-type levels of expression of these proteins. Moreover, although EmrA does not possess any cysteine residues, the putative dimer could be dissociated upon treatment with 4 M β-mercaptoethanol, with only the 45-kDa band apparent after treatment (Fig. 2*B*, *lane 1*). Dissociation of the dimer was presumably due to solvent effects, because the concentration of β-mercaptoethanol required to destabilize the dimer (*e.g.* >2 M) was much greater than normally used to reduce disulfide bridges (*e.g.* 0.1 M) and the dimer could also be dissociated with 4 M Me_2SO (data not shown). In some preparations we noted the presence of a third predominant band with a molecular mass of >100 kDa, suggestive of a trimer. However, this band was not present in all preparations, just in the most concentrated protein preparations, and it tended to disappear after extensive dialysis. This suggested that the monomer, dimer, and trimer are in a concentration-dependent equilibrium. To investigate this possibility further, we introduced a second elution step into the EmrA-(1–390) protein purification procedure, eluting the protein from the nickel-agarose column first with 250 and then 400 mM imidazole and analyzing the samples by SDS-PAGE before dialysis. Our rational was that the trimer, which would have three Ni^{2+}-binding sites, would be held more tightly by the nickel-agarose than the monomer and dimer and would elute preferentially with 400 mM imidazole. Adopting this refined purification protocol; we found that, following a 2-ml wash with 250 mM imidazole, the eluted protein was most concentrated in the first 1-ml elution with 400 mM imidazole. Although the trimer was clearly apparent in this elution fraction (Fig. 2*C*, *lane 2*), the monomer and dimers were also at a higher concentration than in the preceding or subsequent fractions. As with the dimer, 4 M β-mercaptoethanol dissociated the trimer, with only the monomer band apparent on SDS-PAGE (data not shown). To assess the possibility that the oligomerization of EmrA was in fact SDS-induced aggregation of the protein, we also ran the EmrA-(1–390) protein on native PAGE (7.5% polyacrylamide gels/Tris-glycine buffer (pH 7.5)), upon which at least three bands were visible (Fig. 2*D*), indicating that the oligomerization of EmrA-(1–390) is not an artifact of the SDS treatment. As a further test for dimerization, EmrA-(1–390) was subjected to gel chromatography, which yielded two protein elution peaks, indicative of the monomer and the dimer (Fig.

Downloaded from http://www.jbc.org/ at DURHAM UNIVERSITY on August 29, 2017

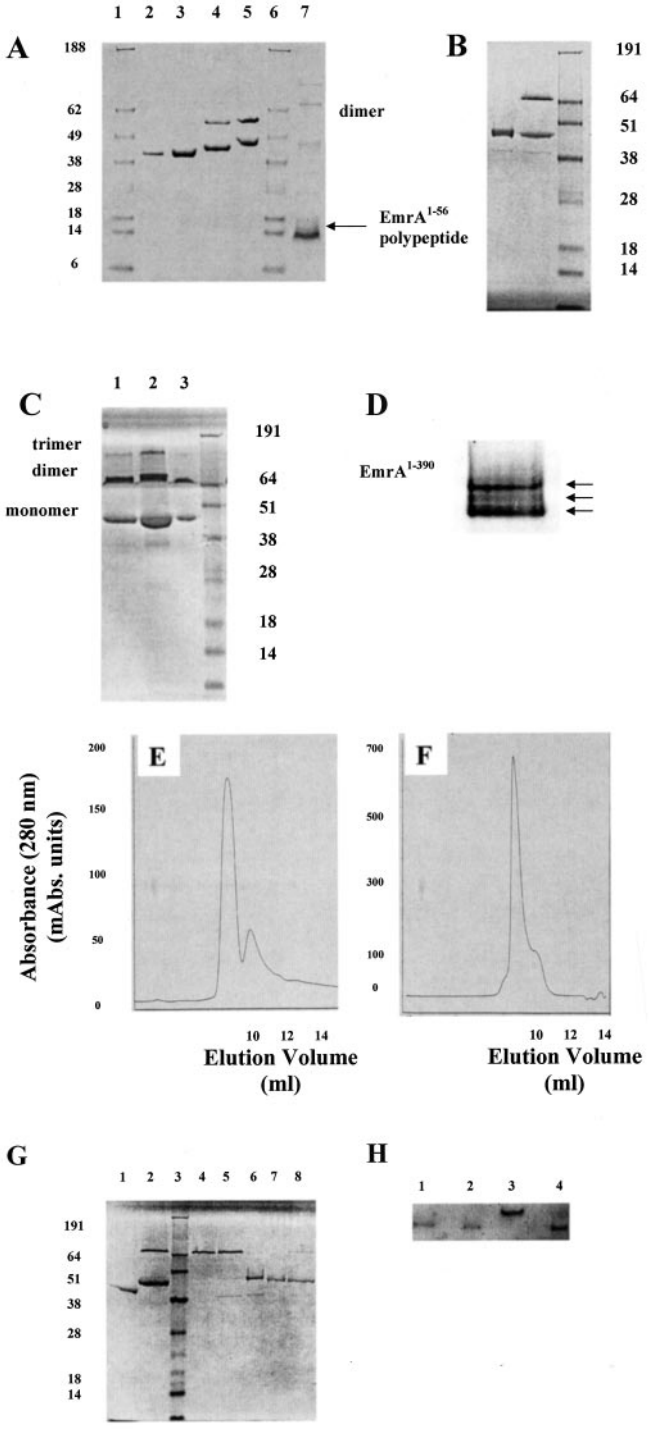

FIG. 2. **EmrA is anchored to the membrane by an N-terminal α-helix that contains a dimerization domain.** *A*, SDS-PAGE (4–12% polyacrylamide gel, MES buffer) analysis of the EmrA proteins: EmrA-(49–390) (*lane 2*), EmrA-(29–390) (*lane 3*), EmrA-(15–390) (*lane 4*), EmrA-(1–390) (*lanes 5*), and EmrA-(1–56) (*lane 7*). EmrA-(29–390), EmrA-(15–390), EmrA-(1–390), and EmrA-(1–56) were isolated from membranes and EmrA-(49–390) from the cytoplasm, consistent with residues 23–46 forming an α-helical membrane anchor. EmrA-(15–390), EmrA-(1–390), and EmrA-(1–56), but not EmrA-(49–390), are shown as forming dimers, demonstrating that this α-helix contains a dimerization domain. Consistent with the presence of a functional leucine zipper in EmrA, EmrA-(29–390), which lacks the first Leu of the putative leucine zipper motif, was membrane-bound but failed to form dimers. *B*, SDS-PAGE (12% polyacrylamide gel, MOPS buffer) analysis of untreated EmrA-(1–390) (*lane 2*) and EmrA-(1–390) treated with 4 M β-mercaptoethanol (*lane 1*), establishing that the higher molecular mass band is a dimer that dissociates when treated with 4 M β-mercaptoethanol. *C*, SDS-PAGE (12% polyacrylamide gel, MOPS buffer) analysis of EmrA-(1–390) eluted from a nickel-agarose column: *lanes 1*, *2*, and *3* are the second 1-ml fraction after the column is eluted with 250 mM imidazole (*lane 1*), the first 1-ml fraction (*lane 2*), and the pooled second to eighth 1-ml fractions (*lane 3*) , respectively, after elution with 400 mM imidazole. The trimer appears concentrated in the first 1-ml fraction eluted with 400 mM imidazole. *D*, a native gel (7.5% polyacrylamide, Tris-glycine buffer (pH 7.5), run at 50 v for 16 h) establishing that EmrA-(1–390) forms oligomers in the absence of SDS (*e.g.* putative monomer, dimer, and trimer bands are indicated by *arrows*). *E* and *F*, separation of EmrA monomers and dimers by gel chromatography. The elution profiles for EmrA-(1–390) (*E*) and EmrA-(49–390) (*F*) eluted from a Superdex 200 column indicate that whereas EmrA-(1–390) exists in both monomeric and dimeric forms, EmrA-(49–390) is predominantly monomeric. *G*, SDS-PAGE (12% polyacrylamide gel, MOPS buffer) analysis of protein samples eluted from the Superdex 200 column: EmrA-(49–390) protein eluting between 10.5 and 11.5 ml (*lane 1*); EmrA-(1–390) protein prior to application to a Superdex 200 column (*lane 2*); EmrA-(1–390) protein eluting between 11 and 12 ml, which had been incubated with the gel buffer for 20 min at 20 °C (*lane 4*) and 75 °C (*lane 5*) and treated with 4 M β-mercaptoethanol (*lane 6*); EmrA-(1–390) protein eluting between 12.5 and 14 ml (*lane 8*) and the same protein heated to 75 °C for 20 min in the presence of 4 M β-mercaptoethanol (*lane 7*). *H*, Western blot, using anti-polyhistidine antibodies, of the purified protein fractions from the Superdex 200 column: the putative EmrA-(1–390) monomer eluting between 12.5 and 15 ml before (*lane 1*) and after (*lane 2*) treatment with 4 M β-mercaptoethanol; and the putative dimer, eluting between 10.5 and 12 ml, before (*lane 3*) and after (*lane 4*) treatment with 4 M β-mercaptoethanol.

2*E*). The two proteins separated by gel chromatography were confirmed as the monomer and dimer by SDS-PAGE (Fig. 2*G*), and the dimer dissociated in the presence of 4 M β-mercaptoethanol (Fig. 2*G*, *lane 6*). Consistent with the identity of each protein as T7-EmrA-(2–390)-His_6, both the monomer and dimer cross-reacted with anti-polyhistidine antibodies (Fig. 2*H*), indicating that both proteins had a C-terminal His tag, whereas N-terminal protein sequencing confirmed that both proteins carried an N-terminal T7 tag. From these experiments we concluded that EmrA-(1–390) forms dimers and trimers.

The N Terminus of EmrA Contains a Leucine zipper Motif That Is Important for Dimerization—In contrast to EmrA-(1–390), soluble EmrA-(49–390) migrated as a single band with an apparent molecular mass of 40 kDa, consistent with the calculated molecular mass of 39.6 kDa (Fig. 2*A*, *lane 2*). Furthermore, EmrA-(49–390) predominantly eluted as a single protein peak from a gel chromatography column, consistent with its monomeric form (Fig. 2*F*). The slight shoulders on either side the central protein peak are probably attributable to small amounts of the dimer and a lower molecular mass-contaminating protein, which can be detected on Coomassie-stained gels generally overloaded with EmrA proteins. We note that the size of the contaminating protein is dependent upon the EmrA truncate that it accompanies, being larger for EmrA (1–390) than EmrA-(49–390), suggesting that it is a product of proteolytic degradation of EmrA. These findings are consistent with the prediction that residues 23–46 form a membrane-spanning α-helix that anchors EmrA to the membrane. The finding that EmrA-(1–56) was exclusively membrane-bound provides further evidence to support our conclusion (Fig. 2*A*, *lane 7*). There is a predominant band that migrates with an apparent molecular mass of about 12 kDa, suggestive of an EmrA-(1–56) dimer because the calculated molecular mass of the monomer is 8.8 kDa. This behavior suggested that EmrA-(1–56) contains a dimerization domain and provided a plausible explanation for the fact that the EmrA-(49–390) protein migrates as a single band (Fig. 2*A*, *lane 2*), whereas two bands are clearly apparent for EmrA-(1–390) (Fig. 2*A*, *lane 5*) and EmrA-(15–390) (Fig. 2*A*, *lane 4*). Interestingly, we noted that the sequence for the N-terminal α-helix that anchors EmrA to the membrane contains a consensus sequence for a leucine zipper (*e.g.* counting from Leu^{23} there are Leu, Leu, Ala, and Leu residues positioned at

Downloaded from http://www.jbc.org/ at DURHAM UNIVERSITY on August 29, 2017

intervals of 1, 8, 15, and 22 residues, respectively), which could lead to the formation of a coiled-coil. To test this hypothesis, we truncated EmrA at position 29, to produce a protein that would still retain most of the α-helix and therefore would be expected to be membrane-bound but would lack the first leucine of the zipper motif, weakening the dimer interactions. Consistent with our hypothesis, the EmrA-(29–390) protein was monomeric and predominantly membrane-bound, migrating as a single band to a position similar to that of the smaller EmrA-(49–390), presumably because EmrA-(29–390) is a membrane protein (Fig. 2*A, lane 2*). We conclude that membrane association alone is insufficient to drive dimerization and that the EmrA-(29–390) construct lacks a functional dimerization domain.

Characterization of the Periplasmic Domain of EmrA—We used the secondary structure prediction program Jpred (24), which indicated that the periplasmic domain of EmrA consists of a large α-helix, comprising residues 96–213, sandwiched by β-sheet structure at the N- and C termini; overall the periplasmic domain has a 37.5% α-helix and a 23% β-sheet structure. To test this latter prediction, we determined the CD spectra for the EmrA-(49–390) protein, which was predicted to have 31% α-helix and 20.1% β-sheet (Fig. 3*A*). Considering the possible errors in determining the protein concentration and their effect upon the CD analysis, this analysis is consistent with the secondary structure prediction from Jpred. We also analyzed the sequence using the program COILS (25), which predicted that residues 95–144 and 156–182 could form the two helices of a coiled-coil. These helices are shorter than the helical region predicted by Jpred because of the presence of proline residues at positions 148 and 197, which are excluded from the helices predicted by COILS. Furthermore, the MULTICOIL (26) program predicted that these helices would form dimers and, with a higher probability, trimers. Consistent with this prediction, we found that under native PAGE conditions, a concentrated sample of EmrA-(49–390) formed oligomers (data not shown), indicating a propensity of the periplasmic domain to oligomerize; but presumably these contacts are less stable than those in EmrA-(1–390) because we do not see oligomers of EmrA-(49–390) on SDS-PAGE unless the gel was severely overloaded with the protein. Furthermore, the insertion of cysteine residues at the N- and C-terminal ends of EmrA-(49–390) stabilized the formation of dimers and trimers by the periplasmic domain, which were readily identified by SDS-PAGE.[2]

If EmrA-(49–390) has two distinct domains, an α-helical coiled-coil domain and a β-sheet domain, the stability of these domains might differ under progressively denaturing conditions, such as increasing GdmCl concentrations. Consistent with this prediction we found that the CD signal at 222 nm, indicative of the α-helical content of the protein, underwent a sharp transition (*e.g.* midpoint ~ 1.125 M) to a lower level with increasing concentrations of GdmCl, probably because of the highly cooperative unfolding of the α-helical coiled-coil (Fig. 3*B*). Moreover, analysis of the individual CD traces using the secondary structure prediction program SELCON indicated, in contrast to the β-structure, a decrease in the α-helical content of the protein with an increasing GdmCl concentration, consistent with the predicted two-domain structure.

We decided to test whether EmrA might also be an elongated molecule, consistent with the predicted structure of a β-barrel attached to a long α-helical coiled-coil. Analytical ultracentrifugation was used to analyze the protein shape. First, a sedimentation equilibrium analysis was used to assess the oligomeric state of EmrA-(49–390). These measurements indicated that the protein is monomeric, with an average molecular mass of 41 kDa, which is consistent with the calculated value of 39.6 kDa. To assess the symmetry of EmrA-(49–390), we measured the sedimentation coefficient ($s^0_{20,w}$), which was found to be 2.19 S at 20 °C, yielding a value for the Stokes radius (R_s) of 4.30 nm. In contrast, if EmrA-(49–390) was a compact sphere, it should have a radius of 2.3 nm. These sedimentation data thus suggest that EmrA-(49–390) is a highly asymmetric protein. To confirm this conclusion, we measured the diffusion coefficient ($D_{20,w}$), which can also be determined from boundary spreading sedimentation velocity data or, more directly, by dynamic light scattering. The dynamic light scattering experiments indicated

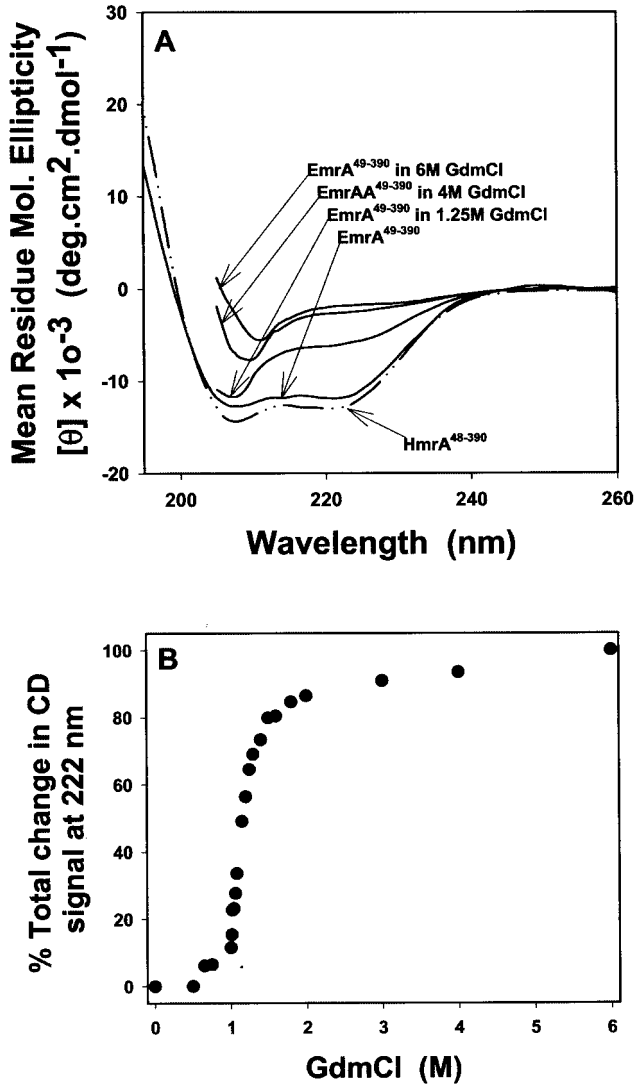

FIG. 3. **CD spectral analysis of EmrA-(49–390) and HmrA-(48–390).** *A*, the CD spectra for EmrA-(49–390) predict a secondary structural content of 31% α-helix and 20.1% β-sheet, consistent with the Jpred prediction of a periplasmic domain consisting of an α-helical coiled-coil domain (37.5%) and a β-sheet domain (23%). The CD spectra for EmrA-(49–390) in the presence of GdmCl indicate a loss of signal at 222 nm, suggesting that the unfolding of EmrA-(49–390) primarily involves a loss of α-helical content. In contrast, a SELCON analysis indicated that the β-sheet content increased to more than 30% in GdmCl concentrations above 1.25 M, suggesting that the β-sheet domain is more stable than the α-helical coiled-coil. As indicated by the comparable CD spectra, HmrA-(48–390) adopts a structure similar to that of EmrA-(49–390). *B*, unfolding transition of EmrA+. The sharp transition is consistent with the highly cooperative unfolding of the α-helical coiled-coil domain.

[2] M. I. Borges-Walmsley and A. R. Walmsley, unpublished data.

Downloaded from http://www.jbc.org/ at DURHAM UNIVERSITY on August 29, 2017

TABLE I

Hydrodynamic parameters for the periplasmic domain of EmrA (EmrA-(49–390))

The conformational parameters, calculated using the experimentally obtained molecular mass and partial specific volume ($\bar{v}$), were: $s^0_{20,w}$, sedimentation coefficient; $D_{20,w}$, diffusion coefficient; R_s, Stokes radius; f and f_0, fractional coefficients of EmrA-(49–390) and a sphere with a volume equal to EmrA-(49–390); a/b, the axial ratio, where a is the long semi-axis and b is the short semi-axis of a prolate ellipsoid.

	Parameters							
	$s^0_{20,w}$	R_s	$D_{20,w}$	R_h	f/f_0	a/b	$2a$	$2b$
	$s \times 10^{13}$	*nm*	$10^7 \times cm^2\ s^{-1}$	*nm*			*nm*	*nm*
Value	2.19 (±0.05)	4.3	5.45 (±0.05)	4.7	1.86	11.6	27	2.3

a value for $D_{20,w}$ (1 mg ml^{-1} protein) of 4.5 × 10^{-7} cm^2 s^{-1}, which compares with a value of 5.5 × 10^{-7} cm^2 s^{-1} from boundary spreading sedimentation velocity data, and gave a measure of the hydrodynamic radius (R_h) of the protein of 4.7 nm, which is highly comparable with the measured R_s value of 4.3 nm. Assuming EmrA-(49–390) is a prolate ellipsoid, it is possible to calculate the axial ratio and estimate the protein dimensions (Table I). EmrA-(49–390) is predicted to have dimensions of 27 × 2.3 nm (*i.e.* 270 × 23 Å) at 20 °C.

EmrA Is Required for Antibiotic Resistance—pUC constructs were used to express EmrA-EmrB and EmrA-(49–390)-EmrA-EmrB in the *E. coli acr* deletion strain, N43, which is highly susceptible to a wide range of antibiotics (17). Although full-length EmrA and -B were able to confer resistance to CCCP, FCCP, DNP, and nalidixic acid but not erythromycin or chloramphenicol, cells expressing EmrA-(49–390)-EmrA and EmrB were as susceptible to these agents as control cells transformed with pUC (Table II). Because the EmrA-(49–390)-EmrA would not be targeted to the membrane, the data indicate that resistance cannot be conferred solely by EmrB. We also tested the homologous genes *hmrA* and *hmrB* from *H. influenzae* for their ability to confer resistance to these agents. Although these genes did not confer resistance to FCCP and CCCP, they were able to confer resistance to erythromycin, indicating that the Hmr transport system was functional in strain N43 (Table II). In this respect, HmrAB is not unique, because expression of VceAB from *V. cholerae* has been shown to confer resistance to drugs, including CCCP, when expressed in a Δ*emrB* strain of *E. coli* (12). Furthermore, the operon encoding VceAB also encodes the OMP VceC, but VceAB expression is sufficient to complement the deoxycholate sensitivity of a Δ*tolC* strain of *E. coli* (12), indicating that these transporters can operate as bi- and tripartite systems. Indeed, recent studies have shown that the MexJK efflux pump of *Pseudomonas aeruginosa* does not require the OMP OprM for efflux of the biocide triclosan, but it is required for efflux of the antibiotics tetracycline and erythromycin (27).

The Periplasmic Domain of EmrA Binds Transported Drugs—A potential role for EmrA is in the binding of drugs exiting EmrB for transfer to TolC. In this case it might be possible to detect the binding of drugs by fluorescence spectroscopy if any of the four tryptophan residues present in the periplasmic domain were to change environment upon drug binding. Unfortunately it is not possible to monitor the interaction of these drugs with EmrA directly from changes in the tryptophan fluorescence because they all produce a significant inner filter effect that obscures any change in tryptophan fluorescence. However, the exposure of the tryptophan residues of a protein can be assessed by their accessibility to quenching by potassium iodide (28). The binding of a drug to EmrA might be detected as a change in the exposure of the tryptophan residues resulting from a conformational change. Consequently, as an alternative to direct measurements of drug induced changes in the tryptophan fluorescence, we determined the exposure of the tryptophan residues in the absence and presence of drugs. If the protein is titrated with KI, monitoring the quench in fluorescence, the data can be analyzed as a Stern-Volmer plot of F_0/F *versus* the KI concentration, where F_0 and F are the fluorescence of the protein in the absence and presence of KI, respectively (29). A linear plot is indicative of a single class of quenchable tryptophan, but a downwardly curved plot indicates that there are tryptophan residues that differ in their accessibility to KI (28). As shown in Fig. 4*A*, the Stern-Volmer plot for the KI quenching of EmrA-(49–390) was convex to the abscissa, indicating that the four tryptophan residues present in EmrA-(49–390) differ in their accessibility to KI. Clearly, in the presence of the transported drugs FCCP, CCCP, DNP, and nalidixic acid, the exposure of the tryptophan residues was reduced, indicating that the binding of these drugs caused a conformational change in EmrA. In contrast, chloramphenicol, which is not a substrate of the EmrAB transporter, did not appreciably reduce the exposure of the tryptophan residues of EmrA. Although it is unlikely that the nonspecific binding of these drugs would cause a conformational change at the concentrations used, we sought to investigate this possibility using HmrA. It is reasonable to conclude that the HmrA and -B proteins do not interact with FCCP because they do not confer resistance to this drug. However, although the Emr and Hmr transporters differ in their drug specificity, HmrA has 46.2% identity with EmrA, with three of the tryptophans conserved in the two proteins, suggesting that they will adopt very similar structures. Consistent with this prediction, EmrA and HmrA have similar CD spectra (Fig. 3*A*). Accordingly, HmrA-(48–390) was titrated with KI in the absence and presence of FCCP as a control to test for the effects of the nonspecific binding of FCCP. As shown in Fig. 4*B*, a significant difference in the value of F_0/F in the absence and presence of FCCP was apparent only at the highest KI concentration, consistent with a small nonspecific binding effect. To test whether the HmrA was correctly folded and capable of binding transported substrates, the protein was titrated in the presence of erythromycin and nalidixic acid (Fig. 4*C*). Interestingly, we found that HmrA did not behave in an identical manner to EmrA, in that these substrates caused an increase in the F_0/F ratio for HmrA, indicative of an increase in the exposure of the tryptophans due to binding of these substrates. It is possible that this difference results from the binding of drugs in the vicinity of Trp^{76} of EmrA that is not conserved in HmrA.

We used the difference in quenching with 1 M KI, in the presence and absence of FCCP, to titrate EmrA-(49–390) with FCCP (Fig. 5). For low concentrations of FCCP the value for F_0/F decreased in a hyperbolic manner, but as the concentration was increased F_0/F continued to decrease in an apparently linear manner. This behavior is consistent with the specific binding of FCCP at low concentrations but with nonspecific binding becoming apparent at higher concentrations. Accordingly, we analyzed the titration curve by nonlinear regression fitting to an equation incorporating hyperbolic and linear functions; this fitting procedure indicated a maximal quench in the fluorescence of 8.1 (±2.8) % and a K_d for the specific EmrA-(49–390)-FCCP complex of 4.2 (±2.6) μM. The EmrE-FCCP complex has a similar K_d value of 3.0 μM (30). In contrast, when

Downloaded from http://www.jbc.org/ at DURHAM UNIVERSITY on August 29, 2017

TABLE II
The susceptibility of the ΔacrA mutant N43 expressing EmrAB, EmrA-(49–390)-EmrB, and HmrAB to various drugs: MIC measurements for the three N43 transformants

	pUC	pUC-EmrAB	pUC-EmrA-(49–390)B	pUC-HmrAB
	μg ml^{-1}	*μg ml*$^{-1}$	*μg ml*$^{-1}$	*μg ml*$^{-1}$
FCCP	14.8	59.3	14.8	14.8
CCCP	1.9	31.3	1.9	3.9
DNP	11.5	23	11.5	11.5
Nalidixic acid	1.1	8.7	1.1	8.7
Erythromycin	2.3	1.2	1.2	18.4
Chloramphenicol	2.6	2.6	2.6	2.6

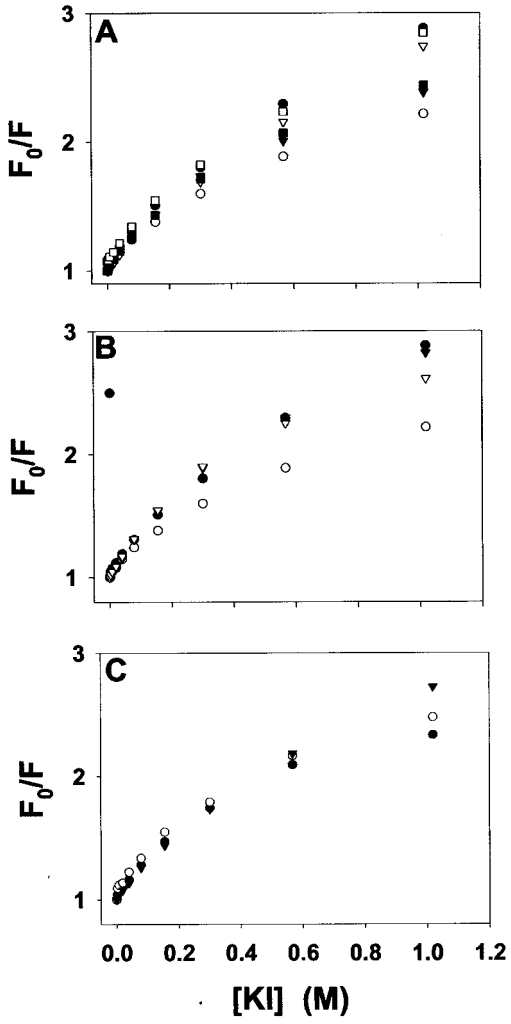

FIG. 4. **The periplasmic domain of EmrA possesses a drug-binding site.** *A*, Stern-Volmer plots for EmrA-(49–390) in the absence (*closed circles*) of drugs and in the presence of 39 μM FCCP (*open circles*), 19 μM DNP (*closed inverted triangles*), 48 μM CCCP (*closed squares*), 20 μM nalidixic acid (*open inverted triangles*), and 53 μM chloramphenicol (*open squares*). The difference in the titration curves is indicative of drug binding, and the lower end points, obtained in the presence of drugs, indicate a decrease in the exposure of the tryptophan residues of EmrA-(49–390) upon binding the drug. Note that chloramphenicol, which is not an Emr substrate, has little effect on the KI titration curve, consistent with the other drugs binding specifically. *B*, Stern-Volmer plots for EmrA-(49–390) (*closed* and *open circles*) and HmrA-(48–390) (*closed* and *open inverted triangles*) in the absence and presence of 39 μM FCCP, respectively. *C*, Stern-Volmer plots for HmrA-(48–390) alone (*closed circles*) and in the presence of 19 μM nalidixic acid (*open circles*) and 17 μM erythromycin (*closed inverted triangles*).

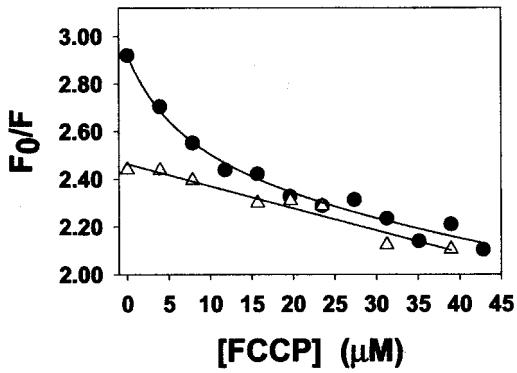

FIG. 5. **Titration of the drug binding site of EmrA.** The fluorescence intensity of EmrA-(49–390) (*closed circles*) and HmrA-(48–390) (*open triangles*) was measured in the presence of the indicated concentrations of FCCP (to give F_0) and after the addition of 1 M KI (to give F). The curve through the EmrA-(49–390) data points is the best-fit obtained by a nonlinear regression fit of the data to an equation with hyperbolic and linear functions, indicating a maximal quench in the fluorescence of 8.1 (±2.8)% and a K_d for the specific EmrA-(49–390)-FCCP complex of 4.2 (±2.6) μM. For HmrA-(48–390), F_0/F decrease in a linear manner, paralleling the behavior of EmrA-(49–390) at high FCCP concentrations, which is indicative of nonspecific binding.

HmrA-(48–390) was titrated with FCCP, F_0/F decreased in a linear manner with increasing FCCP concentration. This behavior parallels that of EmrA-(49–390) at high FCCP concentrations and is consistent with the nonspecific binding of FCCP by HmrA-(48–390) (Fig. 4*C*). A similar analysis yielded K_d values of 1.2 (±1.1) μM and 9.4 (±6.6) μM for the binding of CCCP and DNP, respectively, to EmrA (data not shown),[3] indicative of a correlation between the affinity of EmrA for the drug and the resistance afforded. For example, EmrA binds CCCP with the highest affinity, and this drug is the best substrate for the EmrAB transport system as judged by the increase in the MIC upon expression of the transport system in a Δ*acr* background. We conclude from this analysis that EmrA is a drug-binding protein and is likely to play a role in the direct transfer of drugs from EmrB to TolC.

DISCUSSION

The aim of this study was to characterize EmrA, a membrane fusion protein from a tripartite multidrug extrusion system. By truncating the EmrA protein we were able to show that it is anchored to the inner membrane by residues 1–59, consistent with the proposal that residues 23–46 form a membrane-spanning α-helix, whereas residues 47–390 are arranged into a soluble periplasmic domain. Indeed, we found that EmrA-(15–390) was membrane-bound, whereas EmrA-(49–390) was soluble, indicating that residues 15–48, but not 1–15 or 49–390, are necessary for membrane insertion. Furthermore, EmrA-(29–390) is partially soluble, suggesting that the membrane-spanning helix starts between positions 15 and 29. We predict that the periplasmic domain of EmrA comprises a short β-sheet domain (residues 48–95), a large α-helical domain that is ar-

[3] The fluorescence changes associated with the specific binding of nalidixic acid were too small to be distinguished reliably from those associated with nonspecific binding.

Downloaded from http://www.jbc.org/ at DURHAM UNIVERSITY on August 29, 2017

ranged into a coiled-coil (residues 96–213), and a large β-sheet domain (residues 214–374) with a short C-terminal helix (residues 375–387). This secondary structure prediction is reasonably consistent with a CD analysis of EmrA-(49–390). In common with the MFP AcrA (9) we found that the periplasmic domain of EmrA is highly elongated, with predicted dimensions of 27 × 2.3 nm. EmrA is predicted to have a stretch of 110 residues, with an α-helix structure, which is arranged into a coiled-coil. Assuming that there are 3.5 amino acids/helix turn, with a pitch of 0.51 nm/turn, we would expect this domain to have dimensions of 17 × 2 nm. Thus, both our CD and hydrodynamic data are reasonably consistent with the Jpred secondary structure prediction of a two-domain protein, *e.g.* a globular domain with a largely β-sheet structure capping an α-helical coiled-coil domain.

Herein we provide evidence that membrane-bound EmrA forms dimers and trimers. What is the structural basis for the oligomerization of EmrA? EmrA is predicted to have an α-helical coiled-coil structure, which is a common motif in oligomeric proteins; the MULTICOIL program predicts that the coiled-coil domain will form dimers and trimers. Consistent with this prediction, we found that the soluble periplasmic domain of EmrA (*e.g.* EmrA-(49–390)) formed oligomers (at relatively high protein concentrations), but the dimers formed by membrane-bound whole EmrA (*e.g.* EmrA-(1–390)) were more stable. We note that both membrane-bound and soluble AcrA form dimers and trimers (31). However, AcrA differs from EmrA in that it uses a lipid moiety to anchor it to the inner membrane, indicating that the oligomerization site for AcrA lies within the periplasmic domain. Another MFP, HlyD, was also shown to form trimers (8), suggesting that this is a common feature of MFPs. It seems most likely that a leucine zipper motif that runs through the N-terminal helix of EmrA acts as a dimerization domain, which stabilizes dimers of EmrA-(1–390) relative to those of EmrA-(49–390). Perhaps formation of the dimer provides a scaffold for trimerization, which results from interactions between the periplasmic domains of EmrA. In such a trimer the third leucine zipper motif would be "free." Thus, it is of interest to note that both the putative N-terminal (*e.g.* Leu^{7}, Ile^{14}, Leu^{21}, Leu^{28}, and Val^{35}, which span putative helix 1 between residues 13 and 38) and C-terminal helices (*e.g.* Leu^{473}, Ile^{480}, Ile^{487}, and Leu^{494}, which span putative helix 14 between residues 482 and 504) of EmrB contain leucine zipper motifs, which might interact with the free leucine zipper of the EmrA trimer to form a stable EmrA-EmrB complex. No leucine zipper motifs spanning the other putative helices of EmrB are apparent. Recent studies of HylD indicate that its cytosolic domain mediates transduction of the substrate binding signal to the periplasmic domain to trigger recruitment of TolC (32). Thus, it is inviting to speculate that substrate binding to EmrB triggers communication between EmrB and EmrA via the leucine zippers, with signal propagation to the periplasmic domain of EmrA.

EmrA and TolC are predicted to have similar tertiary and quaternary structures, an elongated α/β-barrel that forms trimers (33). This is suggestive of a related structure and function for these proteins, possibly with both acting to channel drugs across the periplasm. Indeed, the trimeric structure of EmrA is suggestive of the formation of a six-helix barrel, which could form a connecting channel with TolC. However, both TolC and EmrA are predicted to be sufficiently long to span most, if not all, of the periplasmic space, bringing into question how this interaction might be achieved if only the ends of the helical channels are involved. An alternative hypothesis might be one in which each α-helical coiled-coil of trimeric EmrA would act like "arms to grab" TolC, inducing the periplasmic end of TolC to adopt an open confirmation. Consistent with this hypothesis, recent studies indicate that a ring of aspartate residues (34) and an intramolecular salt bridge (35) at the periplasmic end of TolC control the opening of the tunnel; their interaction with the MFP could be used to control the opening of TolC. However, there is evidence that the IMP and MFP, which are coupled, can work independently of the OMP (12, 27). It is possible that the MFP performs a role similar to that of TolC but channels the drugs to the outer membrane. Thermodynamically, the delivery of hydrophobic drugs to the outer membrane would be favorable.

On the basis of the structure of the RND antiporter, AcrB, it has been suggested that the MFP AcrA binds to a large cleft in the periplasmic headpiece of AcrB (5). In this position it would overlap the periplasmic domains of AcrB and TolC, where it could play a role in recruiting TolC. If this is the case, it brings into question the site of interaction of EmrA with EmrB, because EmrB is a major facilitator antiporter (1), which does not possess large periplasmic domains between helices 1 and 2 and helices 7 and 8. Perhaps the leucine zipper motif of EmrA is of importance in the EmrA-EmrB interaction, because it is noticeable that whereas EmrA is anchored by an α-helix, AcrA is anchored to the membrane by a lipid moiety. It has also been suggested that drugs can bind to the headpiece of AcrB and be channeled into the central pore region (5). The headpiece contains vestibules that are open to the periplasm, which could be used to channel drugs to the pore at the center of the headpiece. Drugs delivered to the pore from the periplasm could then be delivered to TolC. Recent studies have shown that swapping the periplasmic domains of the two RND antiporters, AcrB and AcrD, which differ in their drug specificity, results in a change in the drug specificity of the chimeric proteins (36), thus providing evidence that the periplasmic domains of AcrB are involved directly in drug binding. Herein we provide evidence that EmrA binds transported drugs, and it is tempting to speculate that EmrA may serve a similar role to that of the periplasmic domains of RND antiporters in drug binding and transfer to the OMP.

A plausible model for the structure and function of the EmrB-EmrA-TolC tripartite transport system might be one in which EmrB and EmrA form a stable complex, possibly via their membrane-spanning leucine zipper motifs, positioning the β-sheet domain of EmrA above EmrB at the surface of the membrane, with the α-helices radiating out across the periplasm in position to contact TolC when triggered by the binding of drugs to the β-sheet domain of EmrA. The α-helical coiled-coils of EmrA would grab TolC so as to position the α-helical barrel of TolC above the β-sheet domain of EmrA. The drug could then be released from the β-sheet domain of EmrA, allowing it to diffuse into the channel formed by the TolC trimer. Although one can envisage the drug moving from a less hydrophobic site on EmrA/EmrB to a more hydrophobic site on TolC, it is puzzling as to how TolC rids itself of the drug. Clearly a detailed understanding of the function of EmrA will require knowledge of the three-dimensional structure, and toward this end we have recently succeeded in crystallizing EmrA.

REFERENCES

1. Borges-Walmsley, M. I., and Walmsley, A. R. (2001). *Trends Microbiol.* **9,** 71–79
2. Johnson, J. M., and Church, G. M. (1999). *J. Mol. Biol.* **287,** 695–715
3. Andersen, C., Hughes, C., and Koronakis, V. *EMBO Rep.* **1,** 313–318
4. Koronakis, V., Sharff, A., Koronakis, E., Luisi, B., and Hughes, C. (2000) *Nature* **405,** 914–919
5. Murakami, S., Nakashima, R., Yamashita, E., and Yamaguchi, A. (2002) *Nature* **419,** 587–593
6. Dubochet, J., McDowall, A. W., Menge, B., Schmid, E. N., and Lickfeld, K. G. (1983). *J. Bacteriol.* **155,** 381–390

Downloaded from http://www.jbc.org/ at DURHAM UNIVERSITY on August 29, 2017

7. Graham, L. L., Beveridge, T. J., and Naninga, N. (1991) *J. Bacteriol.* **173,** 1623–1633
8. Thanabalu, T., Koronakis, E., Hughes, C., and Koronakis, V. (1998) *EMBO J.* **17,** 6487–6496
9. Zgurskaya, H. I., and Nikaido, H. (1999) *J. Mol. Biol.* **285,** 409–420
10. Lomovskaya, O., and Lewis, K. (1992) *Proc. Natl. Acad. Sci. U. S. A.* **89,** 8938–8942
11. Pao, S. S., Paulsen, I. T., and Saier, M. H. (1998). *Microbiol. Mol. Biol. Rev.* **62,** 1–34
12. Colmer, J. A., Fralick, J. A., and Hamood, A. N. (1998). *Mol. Microbiol.* **27,** 63–72
13. Lee, E. H., and Shafer, W. M. (1999). *Mol. Microbiol.* **33,** 839–845
14. Alonso, A., and Martinez, J. L. (2000). *Antimicrob. Agents Chemother.* **44,** 3079–3086
15. Lin, J., Michel, L. O., and Zhang, Q. (2002) *Antimicrob. Agents Chemother.* **46,** 2124–2131
16. Miroux, B., and Walker, J. E. (1996). *J. Mol. Biol.* **260,** 289–298
17. Ma, D., Cook, D. N., Alberti, M., Pon, N. G., Nikaido, H., and Hearst, J. E. (1993). *J Bacteriol.* **175,** 6299–6313
18. Hunt, A. G., and Hong, J. (1986) *Methods Enzymol.* **125,** 302–309
19. National Committee for Clinical Laboratory Standards (1990) *Methods for Dilution Antimicrobial Susceptibility Tests for Bacteria That Grow Aerobically*. Vol. 10, No. 8, Document M7-A2, National Committee for Clinical Laboratory Standards, Villanova, PA
20. Sreerama, N., and Woody, R. W. (1993). *Anal. Biochem.* **209,** 32–44
21. Philo, J. S. (2000). *Anal. Biochem.* **279,** 151–163
22. Laue, T. M., Shah, B., Ridgeway, T. M., and Pelletier, S. (1992) in *Analytical Ultracentrifugation in Biochemistry and Polymer Science* (Harding, S. E., Rowe, A. J., and Horton, J., eds) pp 90–125, Royal Society of Chemistry, Cambridge, UK
23. Krogh, A., Larsson, B., von Heijne, G., and Sonnhammer, E. L. L. (2001) *J. Mol. Biol.* **305,** 567–580
24. Cuff, J. A., Clamp, M. E., Siddiqui, A. S., Finlay, M., and Barton, G. J. (1998). *Bioinformatics* **14,** 892–893
25. Lupas, A., Van Dyke, M., and Stock, J. (1991) *Science* **252,** 1162–1164
26. Wolf, E., Kim, P. S., and Berger, B. (1997) *Protein Sci.* **6,** 1179–1189
27. Chuanchuen R., Narasaki, C. T., and Schweizer, H. P. (2002). *J. Bacteriol.* **184,** 5036–5044
28. Szabo, A. G. (2000) in *Spectrophotometry and spectrofluorimetry*: *A Practical Approach* (Gore, M. G., ed) pp. 62–66, Oxford University Press, Oxford, UK
29. Eftink, M. R. (1991) in *Topics in Fluorescence Spectroscopy* (Lakowicz, J. R., ed) pp 53–126, Plenum Press, New York
30. Zgurskaya, H. I., and Nikaido, H. (2000) *J. Bacteriol.* **182,** 4264–4267
31. Balakrishnan, L., Hughes, C., and Koronakis, V. (2001) *J. Mol. Biol.* **313,** 501–510
32. Sharff, A., Fanutti, C., Shi, J., Calladine, C., and Luisi, B. (2001) *Eur. J. Biochem.* **268,** 5011–5026
33. Andersen, C., Koronakis, E., Hughes, C., and Koronakis, V. (2002) *Mol. Microbiol.* **44,** 1131–1139
34. Andersen, C., Koronakis, E., Bokma, E., Eswaran, J., Humphreys, D., Hughes, C., and Koronakis, V. (2002) *Proc. Natl. Acad. Sci. U. S. A.* **99,** 11103–11108
35. Brooun, A., Tomashek, J. J., and Lewis, K. (1999) *J. Bacteriol.* **181,** 5131–5133
36. Elkins, C. A., and Nikaido, H. (2002) *J. Bacteriol.* **184,** 6490–6498

Downloaded from http://www.jbc.org/ at DURHAM UNIVERSITY on August 29, 2017

Identification of Oligomerization and Drug-binding Domains of the Membrane Fusion Protein EmrA

M. Ines Borges-Walmsley, Jeremy Beauchamp, Sharon M. Kelly, Kornelia Jumel, Denise Candlish, Stephen E. Harding, Nicholas C. Price and Adrian R. Walmsley

J. Biol. Chem. 2003, 278:12903-12912.
doi: 10.1074/jbc.M209457200 originally published online December 13, 2002

Access the most updated version of this article at doi: 10.1074/jbc.M209457200

Alerts:
- When this article is cited
- When a correction for this article is posted

Click here to choose from all of JBC's e-mail alerts

This article cites 31 references, 14 of which can be accessed free at
http://www.jbc.org/content/278/15/12903.full.html#ref-list-1

Downloaded from http://www.jbc.org/ at DURHAM UNIVERSITY on August 29, 2017